

Time-resolved luminescence quenching in thin films of perylene-tetracarboxylic-dianhydride

R. Schüppel, T. Dienel, K. Leo, and M. Hoffmann *

Institut für Angewandte Photophysik, Technische Universität Dresden, 01062 Dresden, Germany, www.iapp.de

Abstract

We present luminescence quenching experiments and determine the exciton diffusion length in polycrystalline thin films of PTCDA (perylene-3,4,9,10-tetracarboxylic-dianhydride). From an analysis of time-resolved experiments, we can distinguish between exciton transport during an ultra-fast initial relaxation phase and transport in the long-living emitting states. The temperature dependence of the exciton diffusion constant in the emitting states indicates thermally activated hopping.

Key words: PTCDA (perylene-3,4,9,10-tetracarboxylic-dianhydride), organic thin films, time-resolved luminescence, luminescence quenching, exciton diffusion

PACS: 72.20.Ee, 78.55.Kz, 78.66.Qn

1. Introduction

The transport properties of photo-generated excitons in organic semiconductors are important parameters for the development of optical devices, in particular solar cells. We use surface luminescence quenching experiments to determine the exciton diffusion length in PTCDA (perylene-3,4,9,10-tetracarboxylic-dianhydride). In such an experiment, the optically generated excitons diffuse in the investigated donor material until they are quenched by reaching the surface to an acceptor, which in our case is TiOPc (titanyl-

phthalocyanine). In contrast to bulk quenching experiments with acceptor molecules doped into the donor, the surface quenching experiment in general allows to distinguish between the *capture limited* case, where the capture rate at the acceptor is the limiting factor, and the *diffusion limited* case, where the limiting process is the diffusion of the excitons to the acceptor. The assumption of perfect exciton capture at the donor/acceptor interface, which is often made, can lead to an underestimation of the diffusion length [1,2].

Fig. 1 shows a scheme of the considered relaxation and transfer processes. The excited states of PTCDA consist of Frenkel- and Charge-Transfer excitons strongly coupled to molecular vibrations (e.g., [3–7]). For any total momentum k , there is a broad density of mixed states and only the states at $k = 0$ de-

* Corresponding author. Tel.: +49 351 463 32655; Fax: +49 351 463 37065.

Email address: mi-hoffm@iapp.de (M. Hoffmann).

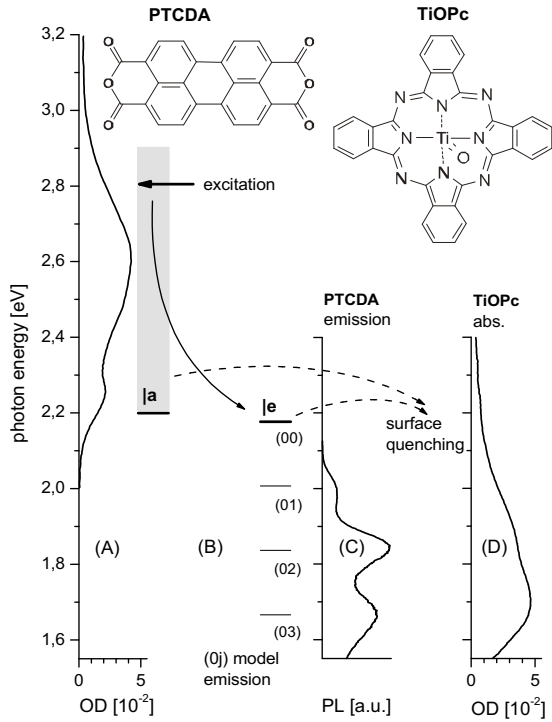


Fig. 1. (A) absorption spectrum of PTCDA polycrystalline thin film, $T=295\text{K}$, thickness 6.3 nm; (B) scheme of three level system, excitation at 2.8 eV to higher vibronic states $|a\rangle$ with total momentum $k = 0$ (light shaded), ultra-fast relaxation to emitting states $|e\rangle$ at the border of the Brillouin zone, luminescence due to transition to the higher vibrational levels ($\hbar\omega = 0.17\text{ eV}$) of the electronic ground state ($|0j\rangle$), the (00) transition is dipole forbidden [4]; (C) transient luminescence spectrum (0...1.6 ns) of PTCDA, $T=5\text{K}$, measured as described in Sec. 3; (D) absorption spectrum of TiOPc thin film, $T=295\text{K}$, acting as a surface quencher.

scribe the absorption spectrum. Caused by the positive sign of the Frenkel transfer integral, the optically forbidden states at the border of the Brillouin zone generally have a lower energy. They are the origin of indirect luminescence transitions to the vibrational levels of the ground state. In the exciton model of Ref. [4], at $T=10\text{ K}$ the lowest absorbing state lies at 2.20 eV and the lowest emitting state 23 meV lower. From the complexity of time-resolved emission spectra, however, it is clear that there is a number of different emitting states related to various minima in the vibrational potential [5] and possibly to the coexistence of different crystal phases in thin films [8]. Comparing our 5 K emission spectrum (Fig. 1C) with Ref. [8], our spectrum seems to be dominated by emission from the

β -crystal phase [8]. The various emitting states result in strongly multi-exponential decay curves with time constants from 100 ps to 60 ns. After optical excitation to $k = 0$ states, the emitting states are populated on a fs time scale even at low temperatures. This is tentatively seen in the luminescence decay curves in Fig. 2 since the luminescence rise time is well below the time resolution of about 5 ps. Pump-probe measurements indicate a time scale of about 100 fs [9].

Because of the large difference in time scales, we distinguish between exciton transport processes during the short initial relaxation phase and exciton transport in the emitting states. This distinction leads to a three-level model ($|a\rangle, |e\rangle, |0\rangle$) for exciton diffusion. The $|a\rangle$ state (“absorbing”) represents all states visited during the initial relaxation process and the $|e\rangle$ state (“emitting”) represents the group of comparatively long living emitting states. In our evaluation of the $|e\rangle$ states, we consider the effective decay and exciton transport dynamics averaged over the first 1.6 ns. At longer time scales, our decay constants become larger (e.g. 48 ns at 5 K evaluated from 1.6 ns to 11.6 ns for the single layer in Fig. 2) and tend to the values reported in Ref. [10]. Since our spectra and time constants are similar to Refs. [8] and [10], resp., we conclude that we observe similar emitting states although we excite at higher energy.

As our evaluation in Sec. 3 shows, both $|a\rangle$ and $|e\rangle$ states can be quenched in the presence of the additional TiOPc layer. The quenching channels and the absorption spectrum are illustrated in Fig. 1. The strong overlap of the TiOPc absorption spectrum with the indirect emission spectrum from the $|e\rangle$ states (Fig. 1C) or with a possible emission from $|a\rangle$ to vibrational levels of the ground state suggests Förster transfer as a quenching mechanism. This is supported by the observation of a weak sensitized TiOPc emission (not shown). However, contributions from electron/hole transfer can not be ruled out.

2. Diffusion in the three-level model

The photoluminescence signal $I(t)$ is given by the spatially integrated exciton density n in the emitting states

$$I_j(t) = \eta \int_0^d n_j(x, t) dx. \quad (1)$$

The subscript j is introduced to distinguish between the single layer experiment ($j = u$, “unquenched”) and the double layer experiment with the additional TiOPc quencher layer on top of the PTCDA ($j = q$, “quenched”). x is the vertical distance from the upper surface of the PTCDA layer (air or quencher) and the substrate is at $x = d$ with d being the PTCDA layer thickness. η includes all outcoupling and detection efficiencies, which we assume to be the same for both single and double layer experiment.

In general, the three-level diffusion problem is now described by two partial differential equations for the excitons in the $|a\rangle$ and $|e\rangle$ states. Here, we consider only the diffusion problem for the long-living $|e\rangle$ state. Its initial population dynamics cannot be directly observed since it takes place on the fs relaxation time scale. After this relaxation phase, there are no $|a\rangle$ state excitons left and we have an initial $|e\rangle$ state exciton density $n_j^0(x)$.

In the double layer experiment, both $|a\rangle$ and $|e\rangle$ state excitons can be quenched. Therefore, the initial $|e\rangle$ state population in the double layer experiment is different from that of the single layer case. This difference shows up as a different initial photoluminescence signal $I_j(0)$ at $t = 0$. It can be read from the experimental decay curves in Fig. 2 if the logarithmic scaling and the offset resulting from the preceding pulses are properly taken into account. We define the experimental initial photoluminescence ratio as

$$\Phi_a = I_q(0)/I_u(0), \quad (2)$$

where the index a refers to the $|a\rangle$ excitons as will be shown below.

If the $|a\rangle$ states would simply relax into the $|e\rangle$ states, the initial conditions after a single instantaneous laser pulse excitation would be given by Beer’s law. For the analysis here, we now neglect the effect of diffusion in the single layer experiment and have

$$n_u^0(x) = N_u \alpha e^{-\alpha x}, \quad (3)$$

where is N_u the number of incident photons per area and α the absorption coefficient. For the double layer experiment, we summarize the effect of diffusion and

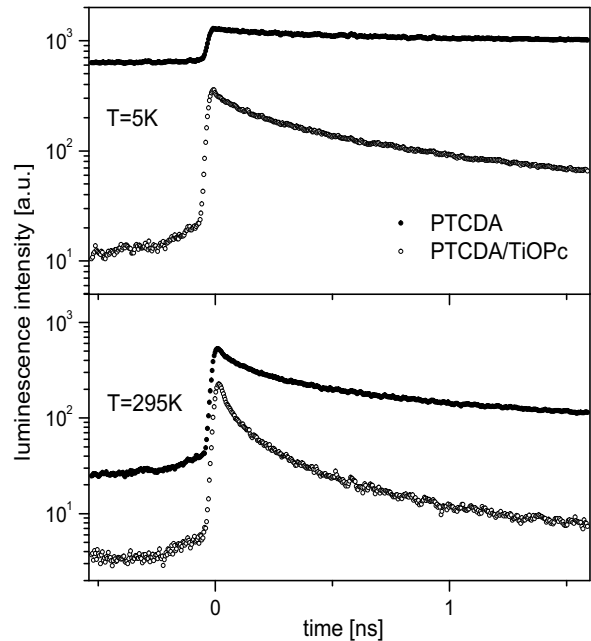


Fig. 2. Time-resolved luminescence of PTCDA thin film (6.3 nm) at (top) $T = 5$ K and (bottom) $T = 295$ K; Full circles: PTCDA single layer, Open circles: PTCDA/TiOPc double layer. The signals are spectrally integrated (1.59-2.07 eV), cf. Fig. 1C. Absolute values are only comparable between the single and double-layer at one temperature.

quenching in the $|a\rangle$ states by regarding a generally reduced initial concentration of excitons in the $|e\rangle$ states:

$$n_q^0(x) = N_q \alpha e^{-\alpha x}. \quad (4)$$

This treatment can account for the fact that a fraction of the $|a\rangle$ -excitons have been lost by quenching ($N_q < N_u$), but still ignores any change of the concentration profile. The advantage of this simple treatment is that the net effect of $|a\rangle$ -exciton quenching is now directly related to the experimentally observable initial photoluminescence ratios by

$$N_q = \Phi_a N_u. \quad (5)$$

The time evolution of the $|e\rangle$ state excitons is governed by the diffusion equation

$$\frac{\partial}{\partial t} n_j(x, t) = \left(D \frac{\partial^2}{\partial x^2} - k \right) n_j(x, t). \quad (6)$$

The rate constant k corresponds to the effective lifetime $k = \tau^{-1}$ of the excitons in the state $|e\rangle$.

The boundary conditions are expressed by the exciton current $\partial n_j / \partial x$ at the various interfaces as follows:

	$x = 0$	$x = d$
single layer ($j = u$)	0	0
double layer ($j = q$)	$-\kappa_q n_q$	0

(7)

Here, the parameter κ_q describes the exciton capture efficiency at the PTCDA/TiOPc interface. An ideal quencher corresponds to $\kappa_q = \infty$ or, equivalently, to $n_q(0, t) = 0$. At the uncovered and the substrate surfaces, we here assume no quenching, i.e. a vanishing exciton current.

Instead of solving the time-dependent Eq. (6), one can discuss the time-integrated exciton densities

$$\tilde{n}_j(x) = \int_0^\infty n_j(x, t) dt. \quad (8)$$

Application of the operator $D\partial^2/\partial x^2 - k$ from Eq. (6) on Eq. (8) yields the stationary diffusion equation

$$\left(D \frac{\partial^2}{\partial x^2} - k \right) \tilde{n}_j(x) = \int_0^\infty \frac{\partial}{\partial t} n_j(x, t) dt = -N_j \alpha e^{-\alpha x}. \quad (9)$$

Here, we have used the initial conditions from Eqs. (3), (4) and $n_j(x, \infty) = 0$. The boundary conditions (7) are still valid. The solution of this equation has the form $\tilde{n}_j(x) = N_j f_j(x)$, where the function f_j depends on the boundary conditions for the respective case ($j = u$ or $j = q$). The time-integrated exciton density $\tilde{n}_j(x)$ is related to the time-integrated luminescence signal $\tilde{I}_j = \int_0^\infty I_j(t) dt$ by $\tilde{I}_j = \eta \int_0^d \tilde{n}_j(x) dx$.

The time-integrated luminescence ratio

$$\tilde{\Phi} = \tilde{I}_q / \tilde{I}_u \quad (10)$$

between single and double layer signal corresponds to a cw luminescence quenching experiment. In our model, it takes the form

$$\tilde{\Phi}(d) = \frac{N_q \int_0^d f_q(x) dx}{N_u \int_0^d f_u(x) dx}. \quad (11)$$

With Eq. (5), $\tilde{\Phi}(d)$ can be split into

$$\tilde{\Phi} = \Phi_a \Phi_e. \quad (12)$$

Here,

$$\Phi_e(d) = \frac{\int_0^d f_q(x) dx}{\int_0^d f_u(x) dx} \quad (13)$$

is the luminescence intensity ratio that would be observed without quenching of the $|a\rangle$ state excitons ($N_q = N_u$). In a typical cw luminescence quenching experiment [2,11], the possible quenching of a precursor state is not considered and the measured time-integrated ratio $\tilde{\Phi}$ is evaluated by the expression for $\Phi_e(d)$ from Eq. (13) or similar diffusion models. Our time-resolved approach now allows to include the different initial condition (n_u^0 vs. n_q^0) for the $|e\rangle$ state excitons caused by the quenching of the $|a\rangle$ -excitons.

3. Experimental results

Our films are vapor deposited on freshly cleaved mica in an ultra-high vacuum system with deposition rates of about 1 \AA min^{-1} . Time-resolved luminescence is measured with a setup consisting of a frequency doubled Ti:sapphire picosecond laser (2.8 eV photon energy, $10^{-7} \text{ J cm}^{-2}$ energy density per pulse, 12.1 ns pulse repetition time), a spectrometer and a streak camera. For temperature-dependent measurements down to 5 K, the samples are kept in helium vapor in a continuous flow cryostat.

From a series of single and double layers with increasing PTCDA film thickness d , we obtained emission decay curves spectrally integrated as in Fig. 2. In particular at low temperature, the luminescence signal from the preceding pulses has not completely decayed at $t = 0$. However, this remaining signal has a much larger decay constant compared to the decay during the initial 1.6 ns and it has to be attributed to different types of emitting states or even trap-like states. In order to use our model with just one emitting state and one decay constant, we assume that this remaining signal stems from a state that does not contribute to the diffusion process anymore. Therefore, it can be considered as a constant background.

From the decay curves, we evaluated the time-integrated intensity ratios $\tilde{\Phi}$ (Eq. (10) with time inte-

gration over the first 1.5 ns) and the initial intensity ratios Φ_a (Eq. (2)). The resulting intensity ratios Φ_e (Eq. (12)) are shown in Fig. 3. These experimental values are compared to a fit according to Eq. (13) with diffusion length L and quenching parameter κ_q as fit parameters. The measured data show a systematic deviation from the diffusion model for layer thicknesses below 5 nm. Even in a more detailed analysis, these effects could not be explained by quenching at the substrate or by the approximation in Eq. (4). Furthermore, for these very thin layers, we also see a systematic decrease of the single layer luminescence decay times. Therefore, we assume that the intrinsic structure of the PTCDA might be affected for very thin layers and we only evaluate the ratios for $d \geq 5$ nm.

An appropriate fit for all temperatures is possible with a fixed quenching parameter of $\kappa_q^e = 0.06 \text{ nm}^{-1}$. This corresponds to an intermediate scenario between diffusion and capture limit. The diffusion length L is between 15 nm for high temperature and 25 nm for low temperature. Although the number of available data points does not yet allow a precise quantitative analysis, the most significant result is a definite quenching ($\Phi_e < 1$) at the largest layer thickness (≈ 25 nm). At this thickness, the initial ratio Φ_a is already close to one which means that only the $|e\rangle$ excitons are quenched.

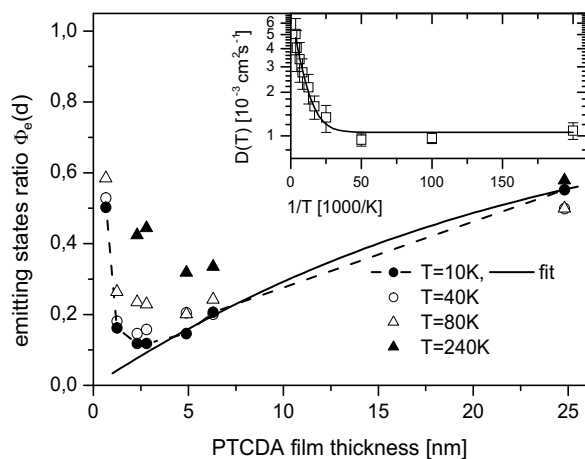


Fig. 3. Intensity ratio Φ_e of the emitting states. An exemplary fit (solid line) according to Eq. (13) is shown for the values at $T=10$ K (dashed line). Inset: Temperature dependence of the diffusion constant D .

From the obtained diffusion length L , we calculate

the diffusion constant $D = L^2/\tau$. For the lifetime τ , we use an effective lifetime of the single layers corresponding to a mono-exponential decay giving the same time-integrated intensity. The resulting $D(T)$ -dependence is shown in the inset of Fig. 3. It can be well described by a fit according to

$$D(T) = D_0 + D_H \exp(-E_H/kT) \quad (14)$$

with activation energy $E_H = 13 \text{ meV}$, $D_H = 6.1 \times 10^{-3} \text{ cm}^2 \text{ s}^{-1}$ and $D_0 = 1.0 \times 10^{-3} \text{ cm}^2 \text{ s}^{-1}$. This thermally activated hopping behavior corresponds to general expectations for exciton transport in molecular crystals with narrow exciton bands (e.g. [12]). The value of D at room temperature has a magnitude comparable to results for polyacene crystals [11]. At low temperatures, we find a temperature-independent diffusion constant D_0 . Theoretically, D can increase again at very low temperatures if the transport becomes coherent and is only limited by phonon scattering (e.g. [12]). This regime is not reached in our case which indicates strong exciton localization caused by strong exciton phonon interaction or by imperfections in the crystal.

Acknowledgement

We thank V. Lyssenko for stimulating discussions. Financial support by the Deutsche Forschungsgemeinschaft (DFG), grant HO 2450/1-1, is gratefully acknowledged.

References

- [1] V. M. Kenkre, Y. M. Wong, Phys. Rev. B **22** (1980) 5716.
- [2] B. A. Gregg, J. Sprague, M. W. Peterson, J. Phys. Chem. B **101** (1997) 5362.
- [3] M. H. Hennessy, Z. G. Soos, R. A. Pascal Jr., A. Girlando, Chem. Phys. **245** (1999) 199.
- [4] M. Hoffmann, Z. G. Soos, Phys. Rev. B **66** (2002) 024305; M. Hoffmann, Z. G. Soos, K. Leo, Nonlinear Optics **29** (2002) 227.
- [5] A. Yu. Kobitski, R. Scholz, I. Vragović, H. P. Wagner, D. R. T. Zahn, Phys. Rev. B **66** (2002) 153204.
- [6] I. Vragović, R. Scholz, Phys. Rev. B **68** (2003) 155202.
- [7] G. Mazur, P. Petelenz, M. Slawik, J. Chem. Phys. **118** (2003) 1423.

- [8] M. Leonhardt, O. Mager, H. Port, Chem. Phys. Lett. **313** (1999) 24.
- [9] E. Engel, M. Koschorreck, K. Leo, M. Hoffmann, in press.
- [10] A. Yu. Kobitski, R. Scholz, D. R. T. Zahn, Phys. Rev. B **68** (2003) 155201.
- [11] R. C. Powell, Z. G. Soos, J. Lum. **11** (1975) 1.
- [12] V. M. Agranovich, M. D. Galanin, Electronic Excitation Energy Transfer in Condensed Matter, North-Holland Publishing Company, Amsterdam, 1982.

Notes to preprint-version added after publication:

Update of Ref.[9]:

- [9] E. Engel, M. Koschorreck, K. Leo, M. Hoffmann, J. Lum. **112** (2005), 299.